Adsorbate-induced absorption redshift in an organic-inorganic cluster conjugate: Electronic effects of surfactants and organic adsorbates on the lowest excited states of a methanethiol-CdSe conjugate

Christopher Liu,[1,a)] Sang-Yoon Chung,[2,b)] Sungyul Lee,[2] Shimon Weiss,[1] and Daniel Neuhauser[1]
[1]*Department of Chemistry and Biochemistry, University of California, Los Angeles, California 90095-1569, USA*
[2]*Department of Applied Chemistry (BK 21), Kyunghee University, Kyungki 449-701, South Korea*

(Received 13 April 2009; accepted 24 September 2009; published online 5 November 2009)

Bioconjugated CdSe quantum dots are promising reagents for bioimaging applications. Experimentally, the binding of a short peptide has been found to redshift the optical absorption of nanoclusters [J. Tsay *et al.*, J. Phys. Chem. B **109**, 1669 (2005)]. This study examines this issue by performing density functional theory (DFT) and time-dependent-DFT calculations to study the ground state and low-lying excited states of $(CdSe)_6[SCH_3]^-$, a transition metal complex built by binding methanethiolate to a CdSe molecular cluster. Natural bond orbital results show that the redshift is caused by ligand-inorganic cluster orbital interaction. The highest occupied molecular orbital (HOMO) of $(CdSe)_6$ is dominated by selenium 4*p* orbitals; in contrast, the HOMO of $(CdSe)_6[SCH_3]^-$ is dominated by sulfur 3*p* orbitals. This difference shows that $[SCH_3]^-$ binding effectively introduces filled sulfur orbitals above the selenium 4*p* orbitals of $(CdSe)_6$. The resulting smaller HOMO-LUMO gap of $(CdSe)_6[SCH_3]^-$ indeed leads to redshifts in its excitation energies compared to $(CdSe)_6$. In contrast, binding of multiple NH_3 destabilizes cadmium 5*p* orbitals, which contribute significantly to the lowest unoccupied molecular orbital (LUMO) of $(CdSe)_6$, while leaving the selenium 4*p* orbitals near the HOMO relatively unaffected. This has the effect of widening the HOMO-LUMO gap of $(CdSe)_6 \cdot 6NH_3$ compared to $(CdSe)_6$. As expected, the excitation energies of the passivated $(CdSe)_6 \cdot 6NH_3$ are also blueshifted compared to $(CdSe)_6$. As far as NH_3 is a faithful representation of a surfactant, the results clearly illustrate the differences between the electronic effects of an alkylthiolate versus those of surfactant molecules. Surface passivation of $(CdSe)_6[SCH_3]^-$ is then simulated by coating it with multiple NH_3 molecules. The results suggest that the $[SCH_3]^-$ adsorption induces a redshift in the excitation energies in a surfactant environment. © *2009 American Institute of Physics*. [doi:10.1063/1.3251774]

I. INTRODUCTION

Modern colloidal preparation methods allow fine control of the optical and electronic properties of II-VI semiconductor nanoparticles.[1–3] The coupling of organic dyes, proteins or DNA to CdSe nanoclusters has produced nanomaterials with sensing, electroluminescent, and therapeutic applications.[4–6] In particular, the bioconjugation of peptides or proteins to CdSe molecular clusters is very promising for fluorescent probes.[7–10]

Experimentally, binding of a short peptide to semiconductor quantum dots redshifts the band gap excitations.[11] This has been attributed to interaction between the exciton and the organic adsorbate.[11] Here this phenomenon is studied using *ab initio* results by simulating the adsorbate-inorganic cluster interaction with a model ligand-cluster complex. The model is built by binding $[SCH_3]^-$, or methanethiolate, to the $(CdSe)_6$ molecular cluster. $(CdSe)_6$ has been experimentally observed by mass spectroscopy[12] and its existence as a colloidal particle has been suggested based on comparison between optical absorption of colloidal clusters and computed highest occupied molecular orbital-lowest unoccupied molecular orbital (HOMO-LUMO) gaps.[13] Several CdSe molecular clusters and their complexes with methanethiolate are examined using density functional theory (DFT) and time-dependent DFT (TDDFT). The results show that the binding of methanethiolate redshifts the excitation energies. Natural bond orbital (NBO) results show that the redshift is caused by the introduction of sulfur 3*p* orbitals that act as hole traps.

Colloidal clusters are synthesized in the presence of surfactants. Without surfactants, it is known that empty cadmium orbitals act as electron traps under the LUMO; these orbitals tend to lower the computed excitation energies compared to the experimental optical gap of passivated molecular clusters.[14] It is therefore interesting to explore how the presence of surfactants affects the *in vacuo* results. The effect of the surfactants is usually treated by: (i) estimating the experimental optical gap empirically,[14] or (ii) application of a surface boundary potential to suppress the surface traps, such as the use of pseudoatoms.[15] However, a recent benchmark

[a)]Electronic mail: chrisliu@chem.ucla.edu.
[b)]Present Address: Department of Chemistry and Biochemistry, University of California, Los Angeles, CA 90095, USA.

study argues that it may be desirable to explicitly include ligand molecules in the calculations.[16]

Here surfactant passivation is simulated by coating the molecular clusters with multiple ammonia molecules. The results show that binding of multiple NH_3 produces effects expected of surfactant passivation, such as the saturation of empty cadmium orbitals and a subsequent blueshift in the excitation energies.[17] NH_3 binding is then used to simulate surface passivation for the conjugated molecular cluster $(CdSe)_6[SCH_3^-]$. The results show that $[SCH_3]^-$ binding also induces a redshift in the excitation energies in a surfactant surrounding. Examination of the frontier orbitals with NBO shows that the redshift in excitation energies occurs because the sulfur orbitals act as hole traps.

The CdSe molecular cluster and the adsorbate studied here are much smaller than the protein-conjugated nanoclusters on which the optical experiments cited above have been done. The size is severely limited by the fully *ab initio* approach adopted here. A different approach is necessary to test how the electronic effects observed here change when the size approaches that of experimentally accessible nanoclusters.

The rest of this article is organized as follows. Section II reviews the methodology and the computational details. Section III discusses the results. Section IV concludes the study.

II. METHODOLOGY AND COMPUTATIONAL DETAILS

A. Computational software

All DFT and TDDFT calculations were done with GAUSSIAN03. The molecules and isosurface were visualized with Visual Molecular Dynamics.[18,19] The NBO analysis was done with NBO 3.1 packaged with GAUSSIAN03.[20] The density of states (DOS) plots were produced with GAUSSSUM 2.1.[21,22] All nonstandard basis set options in GAUSSIAN 03 were obtained from the EMSL basis set exchange database.[23]

B. Electronic ground state and vertical excitations

The hybrid version of the Perdew–Burke–Ernzerhof (PBE) functional known as PBE0 is used.[24,25] It performs similarly for both finite molecules and extended solids. This is desirable because the structures studied here have characteristics of both. All binding energies have been corrected for both zero-point energy and basis set superposition error. The TDDFT electronic excitations are treated within the adiabatic approximation with PBE. Generalized gradient approximation (GGA) functionals underestimate the excitation energies but yield correct ordering of excited states.[26] The error is believed to be caused by the wrong asymptotic dependence on distance, which can be important for charge transfer excitations.[26,27]

C. Natural bond method (NBO)

The isosurfaces of the frontier orbitals indicate visually the extent of adsorbate-cluster orbital mixing. The NBO method is also used to transform the one-electron Kohn–Sham orbitals into the basis of orthogonal atomic orbitals (NAO). The coefficients in the NAO basis show the contributions of different atomic orbitals to each molecular orbital. For a detailed account of the NBO method, refer to the original references.[28]

D. Basis set and effective core potential (ECP)

The LANL2DZdp basis set is used for the CdSe molecular cluster.[29] The Hay–Wadt ECP is used to account for the core electrons. The valence shell consists of 12 cadmium electrons and six selenium electrons. For the ligand atoms, the all-electron basis set $6\text{-}31+G^{**}$ was used.[30,31] The use of GGA functionals and LANL2DZ is recently shown to be acceptable for CdSe molecular clusters by a benchmark study which tested a variety of methods, functionals, and basis sets.[16]

The sensitivity of the results to the choice of the functional and the basis set was checked by comparing the equilibrium structures, HOMO-LUMO gaps, and excitation energies obtained with different combinations of basis set and exchange-correlation functional [local-density approximation (LDA), B3LYP, and PBE]. The tests were done for the minimal clusters $(CdSe)_4$ and $(CdSe)_6$ and selected ligand-cluster complexes. The following trends are observed in the test results. Keeping the functional the same, a larger basis set usually shortens the Cd–Se bond length and narrows the HOMO-LUMO gap. While the structural parameters and binding energies depend much less sensitively on the functional/basis set combination, the excitations often change by a few tenths of an eV. This is a known issue for currently available TDDFT methods. Keeping the structure and the basis set the same, the LDA and B3LYP functionals give lower excitation energies than PBE.

Despite the discrepancies in the excitation energies between different functional and basis set combinations, the methanethiolate-induced redshift is obtained for every functional/basis set combination tested in the present study. Each functional/basis set combination tested gives results qualitatively consistent with other main observations discussed in the present study. The results are shown in the supplementary material (SI), Figs. S-1, S-2, and S-3, and Tables S-1 to S-8.[45]

III. RESULTS AND DISCUSSIONS

A. Properties of $(CdSe)_6$

1. *Ground state properties of* $(CdSe)_6$

The molecular cluster is first examined as a reference for comparing the effects of ligand complexation. The description will be brief because the results are very similar to several previous studies. When the structure of $(CdSe)_6$ is relaxed, it becomes more symmetric than the initial wurtzite fragment (Fig. 1). The overall shape and symmetry of the cluster is consistent with the structures reported by previous studies.[12,13,32–34] Comparison with the wurtzite structure shows that the selenium atoms tend to relax outwards, while the cadmium atoms tend to move inwards. These features

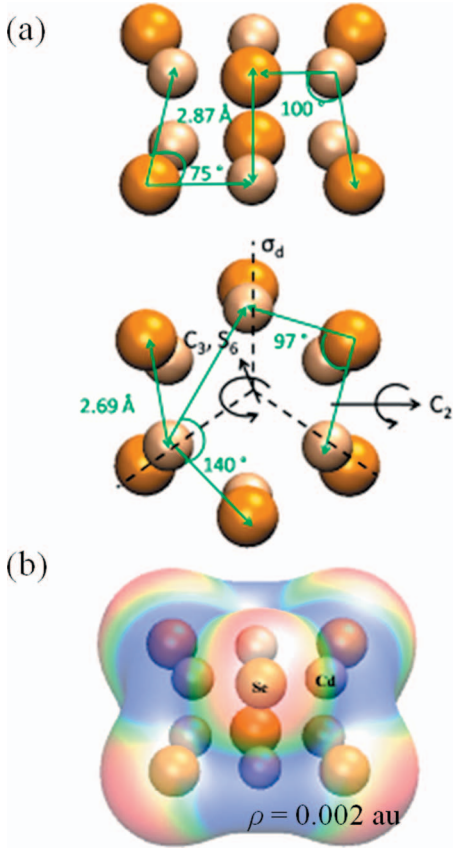

FIG. 1. Atoms are colored with the CPK scheme. (a) Relaxation flattens the layers perpendicular to the *c*-axis. (b) The electrostatic potential is negative (red) around the selenium atoms and positive (blue) around the cadmium atoms.

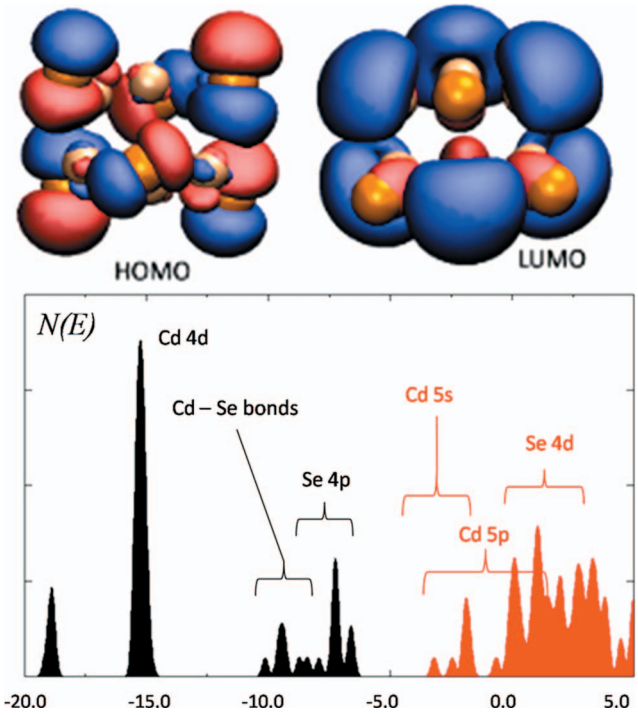

FIG. 2. The DOS is shown near the frontier orbitals of $(CdSe)_6$. The occupied orbitals are black; the empty orbitals are red. The DOS has been broadened by 0.3 eV.

may be observed in the depictions of $(CdSe)_6$ in Puzder *et al.*[34] The wurtzite Cd–Se bond length is about 2.63 Å.[13] When the LANLDZdp basis set and the PBE functional are used, there are two groups of Cd–Se bond lengths in $(CdSe)_6$. On the same (0001) plane, the Cd–Se bond length is 0.02 Å longer. The Cd–Se bond length between different (0001) planes is 0.17 Å longer. This is different from the bond length contraction reported by Puzder *et al.*[34] However, the x-ray diffraction measurements by Jose *et al.*[13] suggest that the Cd–Se bond length is 0.04 Å longer in the molecular clusters than in the wurtzite structure.

Figure 2 shows the DOS of the orbitals near the HOMO-LUMO gap, labeled by the major types of natural atomic orbitals that contribute to those orbitals. The HOMO-LUMO gap is 3.81 eV. This is significantly larger than the HOMO-LUMO gaps obtained by Puzder *et al.*[34] using LDA. Test results show that LDA tends to give lower HOMO-LUMO gaps than B3LYP or PBE; see supporting information, Table S-3.[45] The DOS profile around the frontier orbitals roughly resembles that of the same cluster reported by Puzder *et al.*,[34] especially near the LUMO.

The isosurface plot indicates that the LUMO points along the dangling bond directions, as shown in Fig. 2. NBO analysis indicates that the LUMO is 46% cadmium 5*s* and 26% cadmium 5*p* orbitals. The unsaturated orbitals are therefore mainly cadmium orbitals (Fig. 3). The HOMO consists mainly of selenium 4*p* orbitals. The nature of the orbitals around the HOMO-LUMO gap is consistent with findings obtained from optical experiments of CdSe molecular clusters.[1,35] The agreement is encouraging as it shows that the Kohn–Sham orbitals correctly describe the one-electron orbitals most active in electron transfer and excitations.

2. Excited state properties of $(CdSe)_6$

The first two singlet excited states are degenerate (2.9 eV). Both excited states are forbidden; this is consistent with Troparevsky *et al.*[14] which finds that the first allowed

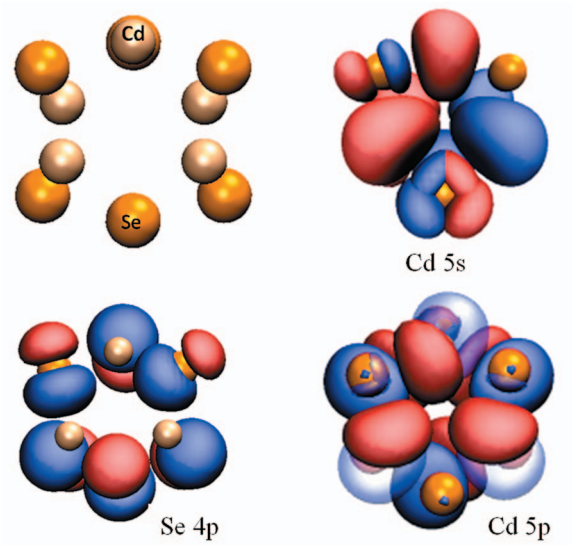

FIG. 3. Selenium 4*p* orbitals dominate the $(CdSe)_6$ HOMO. Cd–Se antibonding orbitals, consisting mainly of cadmium 5*s* orbitals and cadmium 5*p* orbitals dominate the $(CdSe)_6$ LUMO.

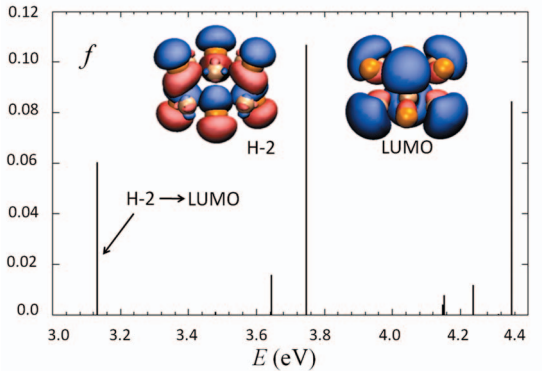

FIG. 4. The absorption spectrum of $(CdSe)_6$ is displayed. Only singlet excitations are shown. The first allowed excitation is from H-2 to LUMO.

excitations are often weak. The first comparatively stronger excitation is at 3.1 eV. The components show that it is an H-2→LUMO excitation (Fig. 4). Most of the excitations originate from the highest occupied orbitals to the LUMO. According to the NAO contributions of the frontier orbitals, the first allowed excitations transfer charge from selenium 4*p* orbitals to cadmium 5*s* or 5*p* orbitals. The direction of electron transfer is the same as known from experiments.[35] The first excitation energy is slightly lower than the first peak in the TD-LDA spectrum obtained by Troparevsky *et al.*[14] However, it is basically identical to the HOMO-LUMO excitation energy assigned by Jose *et al.*[13]

B. Simulation of surfactant passivation with NH_3

Surfactants are stabilizers present in the synthesis of colloidal clusters.[36] It is therefore interesting to examine their effect on the electronic structure of molecular clusters. The most common monodentate surfactants are amines, phosphines, and phosphine oxides. The binding of a typical surfactant is therefore studied here using OPH_3, PH_3, and NH_3. The results show that the surfactants bind to cadmium atoms but not selenium atoms; this has been also reported in a previous study.[16] The binding distances and energies are provided in the supporting information, Table S-5.[45] They are consistent with a previous study on periodic surface facets (Table S-5).[37] Binding of a single NH_3 molecule does not change the nature of the frontier orbitals compared to bare $(CdSe)_6$. The HOMO-LUMO gap increases by less than 0.1 eV (Fig. 5). The lack of orbital interaction near the frontier orbitals is due to the much wider gap of the organic molecule. The excitation energies are only slightly blueshifted from $(CdSe)_6$.

However, coating $(CdSe)_6$ with NH_3 molecules leads to substantial changes in the electronic properties. When all six cadmium atoms are bound to NH_3 the HOMO-LUMO gap increases by 0.6 eV; it also increases the oscillator strength several-fold [Fig. 6(a)]. $(CdSe)_6 \cdot 6NH_3$ has three strong excitations a little under 4.2 eV. Interestingly, the strongest excitation of $(CdSe)_6 \cdot 6NH_3$ is five times stronger than the first excitation of $(CdSe)_6$. Coating $(CdSe)_6$ with ammonia

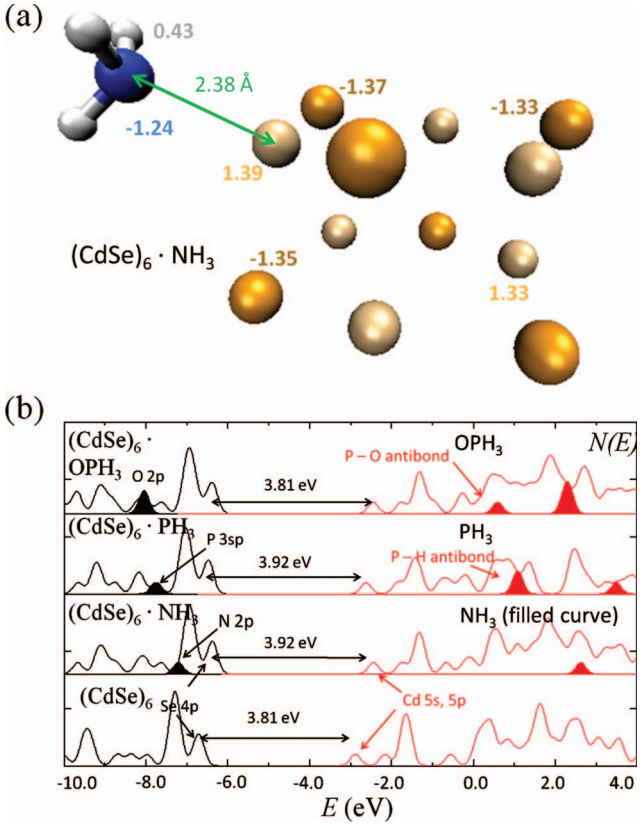

FIG. 5. (a) The equilibrium structures of $(CdSe)_6|NH_3$ is shown along with representative natural atomic charges. (b) The DOSs of $(CdSe)_6$, the adsorbate, and composite are shown for NH_3, PH_3, and OPH_3. In each case, the frontier orbitals of the composite contain similar NAO contributions as those of $(CdSe)_6$. In each case, the adsorbate gap is several eV wider than the cluster.

molecules therefore produces two important effects expected of surfactant passivation: the saturation of cadmium surface states and the blueshift in the excitation energies.

1. *Electronic effects of* NH_3 *binding on* $(CdSe)_6$

As the surface coverage by NH_3 increases, the effects associated with surfactant passivation are also expected to be amplified. Indeed, for $(CdSe)_6 \cdot nNH_3$, the oscillator strength and the excitation energy of the first strongly allowed excitation both increase with *n*, the number of NH_3 [Fig. 6(b)]. Interestingly, as the surface coverage increases, the cadmium 5*p* contribution to the LUMO drops from 26% to less than 1%, as indicated by NBO results. In contrast, the cadmium 5*s* contribution is unaffected, while the antibonding N–H σ^* orbitals of NH_3 slightly increase their contribution[Fig. 6(c)]. As far as NH_3 binding is an accurate model of the surfactant environment, the results suggest that surfactants saturate mainly the cadmium 5*p* orbitals.

The cadmium 5*p* contribution to the LUMO is suppressed because the cadmium orbitals become destabilized by the ammonia molecules. This can be seen as follows. The equilibrium structure shows that the bound ammonia molecule points its lone pair toward the dangling bond of each

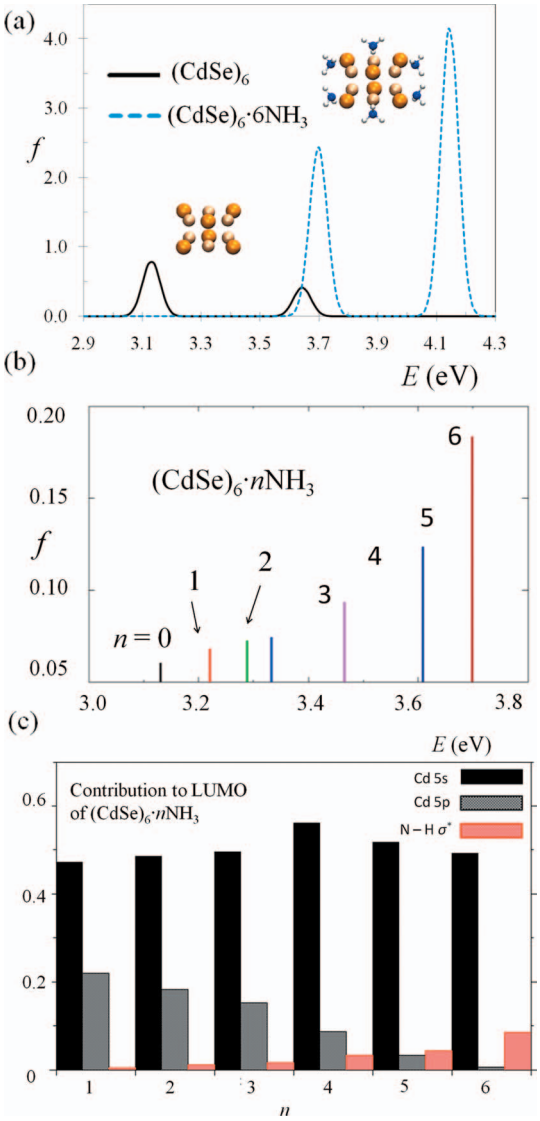

FIG. 6. (a) The excitation energies of $(CdSe)_6 \cdot 6NH_3$ are blueshifted from those of $(CdSe)_6$. The peaks have been broadened by 0.03 eV. Note the intense excitations for $(CdSe)_6 \cdot 6NH_3$ near the experimental onset of $[Cd_4(SePh)_6Cl_4]^{2-}$, which Soloviev *et al.* (Refs. 35 and 38) reported to be 4.2 eV. (b) The excitation energy and the oscillator strength of the first excited state increase with the number of NH_3 molecules. (c) The LUMO of $[(CdSe)_6|nNH_3]$ contains a decreasing amount of cadmium 5*p* orbitals as *n* increases.

cadmium atom. This destabilizes the LUMO because its amplitude is large along the dangling bond direction; see Fig. 4. Accordingly, the NBO results show significant electron donation from the nitrogen lone pairs to the cadmium 5*s*/*p* orbitals which make up most of the $(CdSe)_6 \cdot 6NH_3$ LUMO. The cadmium 5*p* orbitals are more destabilized by this electron donation than the 5*s* orbitals; this is possibly due to the fact that the 5*p* orbitals extend further from the cadmium atoms. Overall, the increased contribution from higher energy orbitals, such as ammonia antibonding orbitals, destabilizes the LUMO. On the other hand, the HOMO is essentially unaffected. The net effect is that ammonia widens the HOMO-LUMO gap of $(CdSe)_6 \cdot 6NH_3$ compared to $(CdSe)_6$. Subsequently, the absorption onset of $(CdSe)_6 \cdot 6NH_3$ occurs at a higher energy.

2. Comparison with similarly sized, passivated molecular clusters

The excitation energy of $(CdSe)_6 \cdot 6NH_3$, is reasonably close to the experimental optical gap of the similarly sized, passivated $[NPr_4^+]_2[Cd_4(SePh)_6Cl_4]^{2-}$ cluster studied by Soloviev *et al.*[35,38] Note that each cadmium atom of $[Cd_4(SePh)_6Cl_4]^{2-}$ is passivated by $[Cl]^-$. This reasonable agreement between the excitation energies is expected because NH_3 binding produces a similar passivating effect as chloride binding. To test whether the agreement is fortuitous, the model complex $[Cd_4(SeH)_6Br_4]^{2-}$ is first examined. This slightly different model complex is selected instead because results are available from Behrens *et al.*[39] and Eichkorn and Ahlrichs.[40] It is essentially Soloviev's $[Cd_4(SePh)_6Cl_4]^{2-}$ complex; the only differences are: (i) each phenyl group Ph is replaced with H; (ii) each halide anion is changed from Cl^- to Br^-. The bond lengths and angles obtained here are comparable to the values reported by the above cited studies. The details are given in SI, Figure S-4 and Table S-9.[45]

Second, Soloviev's $[Cd_4(SePh)_6Cl_4]^{2-}$ complex[38] is studied using the model complex $[Cd_4(SeCH_3)_6Cl_4]^{2-}$. The structure of $[Cd_4(SeCH_3)_6Cl_4]^{2-}$ is given in SI, Figure S-5 and Table S-10.[45] With PBE as the functional, the HOMO-LUMO gap of $[Cd_4(SeCH_3)_6Cl_4]^{2-}$ is 5.13 eV and strong excitations occur near 4.4 eV, which is 0.2 eV higher than the optical gap of $[Cd_4(SePh)_6Cl_4]^{2-}$ reported by Soloviev *et al.*[35,38] As a result, the excitation energies of the well passivated clusters are at least qualitatively reproduced by the methods used here. The excitation energies and oscillator strengths of $[Cd_4(SeCH_3)_6Cl_4]^{2-}$ are given in SI, Table S-12.[45]

C. The electronic effects of alkylthiolate binding

1. Effects of methanethiolate binding on $(CdSe)_6$

Methanethiol (CH_3SH) is used to simulate the effect of a small peptide. Methanethiol forms the side chain of the amino acid cysteine, which is the peptide residue that forms covalent attachment to II-VI semiconductor clusters.[41,42] The thiol group binds more strongly when it is deprotonated ($CH_3SH \rightarrow [CH_3S]^-$), while molecular clusters tend to be neutral.[43,44] This suggests an examination of methanethiolate $[CH_3S]^-$ binding to $(CdSe)_6$

$$(CdSe)_6 + [CH_3S]^- \rightarrow (CdSe)_6[CH_3S]^-.$$

The alternative binding of methanethiol, CH_3SH, is also considered. The results show that the binding energy of $[CH_3S]^-$ is about 2.3 eV higher than CH_3SH. This suggests that protonation of $(CdSe)_6[CH_3S]^-$ is likely to dissociate the adsorbate from the molecular cluster.

The partial charge of the sulfur atom in $(CdSe)_6[CH_3S]^-$ is $-0.6e$; this suggests the excess electron is distributed mostly on the sulfur atom. The charge state of $(CdSe)_6[SCH_3]^-$ is justified by the following: First, the ionization energy of $(CdSe)_6[SCH_3]^-$ is 3.9 eV. Second, ionization to $(CdSe)_6[SCH_3]$ reduces the binding energy by about 2 eV. The Cd–S bond length is 2.5 Å and very close to bulk CdS distance (Fig. 7). The Cd–S bond is formed by a cadmium 5*s*-sulfur 3*p* bond, which is 86% polarized toward

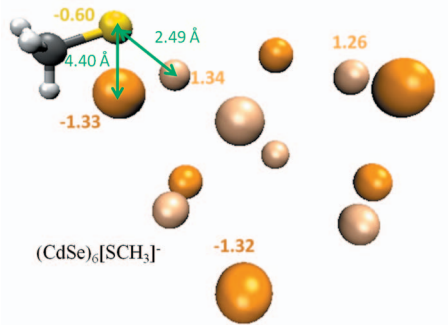

FIG. 7. The equilibrium structure of $(CdSe)_6[SCH_3]^-$ is shown along with representative atomic charges.

sulfur. The binding energy is 2.83 eV. These results indicate an adsorbate-cluster valence bond, supporting the notion that one can attach an organic material via a Cd–S bond.

Methanethiolate binding produces very different effects compared to those produced by coating $(CdSe)_6$ with NH_3 molecules. While the $(CdSe)_6[SCH_3]^-$ LUMO contains a similar composition of cadmium $5s$ and $5p$ orbitals as $(CdSe)_6$, the $(CdSe)_6[SCH_3]^-$ HOMO is very different from the $(CdSe)_6$ HOMO. The NBO results show that the sulfur $3p$ orbitals dominate the $(CdSe)_6[SCH_3]^-$ HOMO and contribute significantly to the first few occupied orbitals below it (Fig. 8). In particular, the localized Cd–S bonding orbital

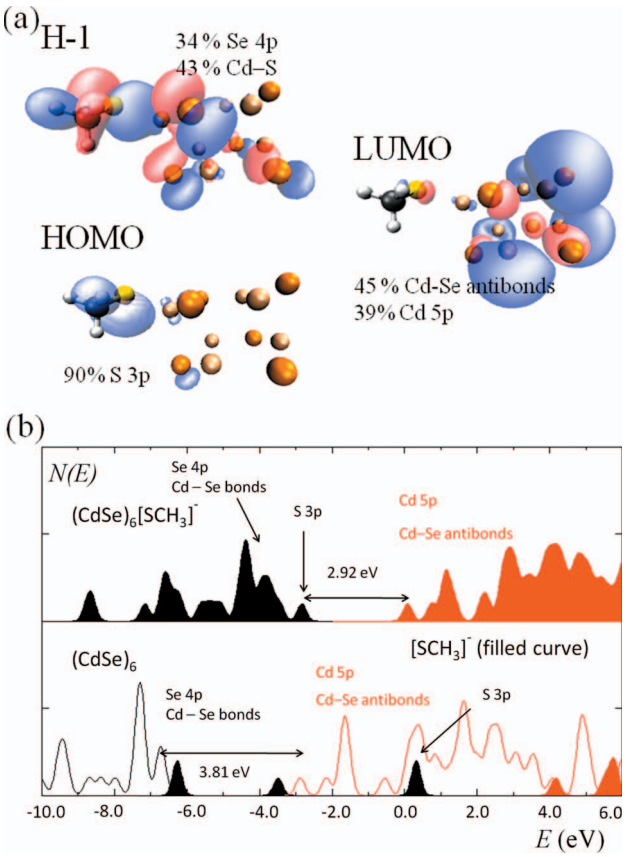

FIG. 8. (a) The isosurfaces of the frontier orbitals of $(CdSe)_6[SCH_3]^-$ show spatial features in agreement with the NBO components. (b) The DOS $N(E)$ of $(CdSe)_6[SCH_3]^-$ is shown in the top panel. The DOSs of $(CdSe)_6$ and $[SCH_3]^-$ (filled curves) are superimposed in the bottom panel. The Cd–Se antibonds are 80% made of cadmium $5s$ orbitals.

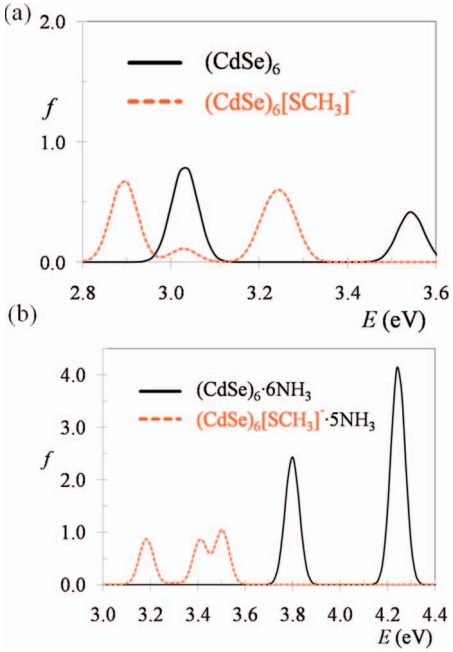

FIG. 9. (a) The excitation energies of $(CdSe)_6[SCH_3]^-$ are redshifted from those of $(CdSe)_6$. (b) The excitation energies of $(CdSe)_6[SCH_3]^-$ $5NH_3$ are redshifted from those of $(CdSe)_6$ $6NH_3$. The peaks have been broadened by 0.03 eV.

makes up one half of H-1. Visually, the isosurface plots show that the highest occupied orbitals have highest amplitudes in the region between the closest cadmium and sulfur pair (Fig. 8).

These results show that the $(CdSe)_6$ HOMO is substantially changed by $[SCH_3]^-$ binding. In particular, the sulfur orbitals of $[SCH_3]^-$ are inserted above the selenium $4p$ orbitals that, before binding, have dominated the $(CdSe)_6$ HOMO. The reason is that the sulfur orbitals are at higher energies than the selenium $4p$ orbitals of $(CdSe)_6[SCH_3]^-$. Effectively, $[SCH_3]^-$ introduces hole traps within the HOMO-LUMO gap of $(CdSe)_6$. Overall, this narrows the HOMO-LUMO gap of the $(CdSe)_6[SCH_3]^-$ compared to $(CdSe)_6$.

In accordance with the smaller HOMO-LUMO gap, the first six excitations of $(CdSe)_6[SCH_3]^-$ are redshifted from the first allowed excitation of $(CdSe)_6$. The first excitation of $(CdSe)_6[SCH_3]^-$ is a forbidden HOMO→LUMO excitation. It is redshifted by the same amount by which the HOMO-LUMO gap of $(CdSe)_6[SCH_3]^-$ is narrowed. The first allowed excitation (f=0.051) is 0.24 eV lower than the first excitation of $(CdSe)_6$ (Fig. 9). It consists of three components: HOMO→LUMO, H-1→LUMO, and H-2→LUMO. This indicates a charge transfer from the sulfur atom to the cadmium orbitals. The excitation creates a hole at the sulfur $3p$ orbital that forms the Cd–S bond. Interestingly, experiments have suggested that photochemical dissociation of thiols is initiated by hole creation at the Cd–S bond.[43]

2. Comparison between $[Cd_4(SeCH_3)_6Cl_4]^{2-}$ *and* $[Cd_4(SeCH_3)_6Cl_3(CH_3S)]^{2-}$

The effect due to adsorption of methanethiolate anion is also tested on $[Cd_4(SeCH_3)_6Cl_4]^{2-}$, the model for Soloviev's

$[Cd_4(SePh)_6Cl_4]^{2-}$-molecular cluster. The $[SCH_3]^-$ is assumed to displace one of the $[Cl]^-$ anion due to the strong Cd–S binding energy

$$[Cd_4(SeCH_3)_6Cl_4]^{2-} + [CH_3S]^- \rightarrow [Cd_4(SeCH_3)_6Cl_3(CH_3S)]^{2-} + Cl^-.$$

The methanethiolate-induced redshift shows up for this molecular cluster as well. For instance, the results obtained with B3LYP show that the HOMO-LUMO gap shrinks by 0.47 eV; the first excitation of $[Cd_4(SeCH_3)_6Cl_3(CH_3S)]^{2-}$ is redshifted by roughly the same amount compared to $[Cd_4(SeCH_3)_6Cl_4]^{2-}$. This test shows that the methanethiolate-induced redshift is not sensitive to the choice for the chemical composition of the colloidal cluster. The structure is given in the supplementary material[45], Figure S-6; and Table S-11; the excitations are listed in Table S-13.

3. Surfactant passivation of $(CdSe)_6[SCH_3]^-$

Coating $(CdSe)_6[SCH_3]^-$ with multiple NH_3 produces similar effects as those discussed above for $(CdSe)_6$. The excitation energies of $(CdSe)_6[SCH_3]^- \cdot 5NH_3$ are blueshifted from those of $(CdSe)_6[SCH_3]^-$. The oscillator strengths also become larger. More interestingly, the HOMO-LUMO gap is shrunk and the excitation energies are redshifted when one NH_3 in $(CdSe)_6 \cdot 6NH_3$ is substituted by $[SCH_3]^-$ according to the reaction

$$(CdSe)_6 \cdot 6NH_3 + [CH_3S]^- \rightarrow (CdSe)_6[CH_3S]^- \cdot 5NH_3 + NH_3.$$

As a result, methanethiolate binding narrows the absorption spectrum of $(CdSe)_6[SCH_3]^- \cdot 5NH_3$ compared to $(CdSe)_6 \cdot 6NH_3$. Further, the magnitude of the redshift is also roughly the same. The first excited state of $(CdSe)_6[CH_3S]^- \cdot 5NH_3$ is forbidden. It is redshifted by 0.7 eV compared to the first allowed excitation of $(CdSe)_6 \cdot 6NH_3$. The first allowed excited state is redshifted by 0.5 eV.

The methanethiolate-induced redshift may therefore be detected even in a surfactant surrounding, as far as it may be simulated by coating the molecular clusters with ammonia. This is perhaps due to the following reason. While multiple ammonia destabilize the $(CdSe)_6[CH_3S]^- \cdot 5NH_3$ LUMO; $[CH_3S]^-$ inserts hole traps above the $(CdSe)_6[CH_3S]^- \cdot 5NH_3$ HOMO. As the two mechanisms work roughly separately from each other, $[CH_3S]^-$ binding redshifts the excitation energies of $(CdSe)_6$ whether the molecular cluster is in gas phase or surrounded by ammonia.

4. Implication for CdSe nanoclusters

The results obtained here are based on molecular clusters. It is unclear whether binding of alkylthiolates will introduce a similar excitation energy redshift for much larger nanoclusters. A nanocluster tends to have a large number of surface traps that lower excitation energies. As a result, the effect of alkylthiolates on the excitation energies might not be distinguishable from that of surface reconstruction. On the other hand, a nanocluster possesses a much larger surface for binding multiple ligands. If the nanocluster has been synthesized so that the surface traps are minimized, then it is reasonable to expect that the sulfur orbitals will behave as hole traps and lower the excitation energies.

IV. CONCLUSIONS

Coating with ammonia molecules blueshifts the optical gap of a CdSe molecular cluster, while the binding of an organic molecule $[SCH_3]^-$ produces the opposite effect. $[SCH_3]^-$ binding narrows the HOMO-LUMO gap and redshifts the excitation energies of the molecular cluster. Binding of multiple NH_3 molecules is used to simulate the surfactant environment for $(CdSe)_6[SCH_3]^-$. In the simulated surfactant surrounding, $[SCH_3]^-$ binding still causes a redshift in the excitations of $(CdSe)_6[SCH_3]^-$ compared to $(CdSe)_6$.

Examination of the NBO results reveals simple reasons for the opposite effects of ammonia versus $[SCH_3]^-$. Coating the molecular cluster with ammonia widens the HOMO-LUMO gap by destabilizing the LUMO. This in turns blueshifts the excitation energies. In contrast, $[SCH_3]^-$ introduces hole traps by inserting filled states above the selenium $4p$ orbitals that dominate the $(CdSe)_6$ HOMO. $[SCH_3]^-$ binding therefore narrows the HOMO-LUMO gap, and redshifts the low-lying excited states of $(CdSe)_6[SCH_3]^-$. While the ammonia molecules induce changes in the LUMO, $[SCH_3]^-$ mainly affects the HOMO. As a result, the redshift induced by $[SCH_3]^-$ is significant even when the $(CdSe)_6[SCH_3]^-$ complex is surrounded by NH_3. As far as ammonia is a faithful model of surfactants used in nanocluster synthesis, these results illustrate how binding of methanethiolate causes a redshift in the excitations of a CdSe molecular cluster.

The observations made here are more immediately applicable to transition metal complexes between small organic molecules and CdSe molecular clusters. The results also have significance for artificially designed peptides that incorporate a CdSe molecular cluster as its active region. Due to the immense computational cost, the largest systems studied here are little more than metal complex containing CdSe molecular clusters. More work, perhaps with a hybrid quantum molecular/molecular mechanics (QM/MM) approach, is necessary to examine whether the methanethiolate-induced redshift verified in this study survive in progressively larger clusters. Nevertheless, the first principles results on the simple models studied here provide extensive evidence that binding of methanethiolate induces a redshift in excitation energies of CdSe molecular clusters.

ACKNOWLEDGMENTS

This work was supported by NSF, Grant No. DMS0835863 (D.N.), NIH Grant No. R01-EB000312 (S.W.). S.L. thanks the financial support by GRRC. C.L. thanks the support of an UCLA Dissertation Year Fellowship.

[1] A. P. Alivisatos, J. Phys. Chem. **100**, 13226 (1996).
[2] L. Manna, E. C. Scher, and A. P. Alivisatos, J. Am. Chem. Soc. **122**, 12700 (2000).

[3] Z. A. Peng and X. Peng, J. Am. Chem. Soc. **123**, 1389 (2001).
[4] M. Artemyev, D. Kisiel, S. Abmiotko, M. N. Antipina, G. B. Khomutov, V. V. Kislov, and A. A. Rakhnyanskaya, J. Am. Chem. Soc. **126**, 10594 (2004).
[5] B. P. Aryal and D. E. Benson, J. Am. Chem. Soc. **128**, 15986 (2006).
[6] J. B. Delehanty, I. L. Medintz, T. Pons, F. M. Brunel, P. E. Dawson, and H. Mattoussi, Bioconjugate Chem. **17**, 920 (2006).
[7] S. R. Whaley, D. S. English, E. L. Hu, P. F. Barbara, and A. M. Belcher, Nature (London) **405**, 665 (2000).
[8] F. Pinaud, D. King, H.-P. Moore, and S. Weiss, J. Am. Chem. Soc. **126**, 6115 (2004).
[9] X. Michalet, F. F. Pinaud, L. A. Bentolila, J. M. Tsay, S. Doose, J. J. Li, G. Sundaresan, A. M. Wu, S. S. Gambhir, and S. Weiss, Science **307**, 538 (2005).
[10] A. M. Smith, G. Ruan, M. N. Rhyner, and S. Nie, Ann. Biomed. Eng. **34**, 3 (2006).
[11] J. Tsay, S. Doose, F. Pinaud, and S. Weiss, J. Phys. Chem. B **109**, 1669 (2005).
[12] E. Sanville, A. Burnin, and J. J. BelBruno, J. Phys. Chem. A **110**, 2378 (2006).
[13] R. Jose, N. U. Zhanpeisov, H. Fukumura, Y. Baba, and M. Ishikawa, J. Am. Chem. Soc. **128**, 629 (2006).
[14] M. C. Troparevsky, L. Kronik, and J. R. Chelikowsky, Phys. Rev. B **65**, 033311 (2001).
[15] X. Huang, E. Lindgren, and J. R. Chelikowsky, Phys. Rev. B **71**, 165328 (2005).
[16] P. Yang, S. Tretiak, A. E. Masunov, and S. Ivanov, J. Chem. Phys. **129**, 074709 (2008).
[17] M. G. Bawendi, M. L. Steigerwald, and L. E. Brus, Annu. Rev. Phys. Chem. **41**, 477 (1990).
[18] M. J. Frisch, G. W. Trucks, H. B. Schlegel *et al.*, GAUSSIAN03, Revision C.02, Gaussian, Inc., Wallingford, CT, 2004.
[19] W. Humphrey, A. Dalke. and K. Schulten, J. Mol. Graphics **14**, 33, (1996).
[20] E. D. Glendening, A. E. Reed, J. E. Carpenter, and F. Weinhold, NBO Version 3.1.
[21] N. M. O'Boyle, A. L. Tenderholt, and K. M. Langner, J. Comput. Chem. **29**, 839 (2008).
[22] http://gausssum.sf.net
[23] D. Feller, J. Comput. Chem. **17**, 1571 (1996).
[24] J. P. Perdew, K. Burke, and M. Ernzerhof, Phys. Rev. Lett. **77**, 3865 (1996).
[25] C. Adamo and V. Barone, J. Chem. Phys. **110**, 6158 (1999).
[26] R. Bauernschmitt and R. Ahlrichs, Chem. Phys. Lett. **256**, 454 (1996).
[27] M. E. Casida, C. Jamorski, K. C. Casida, and D. R. Salahub, J. Chem. Phys. **108**, 4439 (1998).
[28] F. Weinhold, in *Encyclopedia of Computational Chemistry*, edited by P. v. R. Schleyer, N. L. Allinger, T. Clark, J. Gasteiger, P. A. Kollman, H. F. Schaefer, III, and P. R. Schreiner (Wiley, Chichester, 1998), Vol. 3, pp. 1792–1811.
[29] C. E. Check, T. O. Faust, J. M. Bailey, B. J. Wright, T. M. Gilbert, and L. S. Sunderlin, J. Phys. Chem. A **105**, 8111 (2001).
[30] T. Clark, J. Chandrasekhar, G. W. Spitnagel, and P. R. Schleyer, J. Comput. Chem. **4**, 294 (1983).
[31] M. J. Frisch, J. A. Pople, and J. S. Binkley, J. Chem. Phys. **80**, 3265 (1984).
[32] M. C. Troparevsky and J. R. Chelikowsky, J. Chem. Phys. **114**, 943 (2001).
[33] P. Deglmann, R. Ahlrichs, and K. Tsereteli, J. Chem. Phys. **116**, 1585 (2002).
[34] A. Puzder, A. J. Williamson, F. Gygi, and G. Galli, Phys. Rev. Lett. **92**, 217401 (2004).
[35] V. N. Soloviev, A. Eichhofer, D. Fenske, and U. Banin, J. Am. Chem. Soc. **122**, 2673 (2000).
[36] L. Manna, L. Wang, R. Cingolani, and A. Alivisatos, J. Phys. Chem. B **109**, 6183 (2005).
[37] J. Y. Rempel, B. L. Trout, M. G. Bawendi, and K. F. Jensen, J. Phys. Chem. B **110**, 18007 (2006).
[38] V. N. Soloviev, A. Eichhofer, D. Fenske, and U. Banin, J. Am. Chem. Soc. **123**, 2354 (2001).
[39] S. Behrens, M. Bettenhausen, A. C. Deveson, A. Eichhöfer, D. Fenske, A. Lohde, and U. Woggon, Angew. Chem. **108**, 2360 (1996).
[40] K. Eichkorn and R. Ahlrichs, Chem. Phys. Lett. **288**, 235 (1998).
[41] W. C. W. Chan, D. J. Maxwell, X. Gao, R. E. Bailey, M. Han, and S. Nie, Curr. Opin. Biotechnol. **13**, 40 (2002).
[42] S.-Y. Chung, S. Lee, C. Liu, and D. Neuhauser, J. Phys. Chem. B **113**, 292 (2009).
[43] J. Aldana, Y. A. Wang, and X. Peng, J. Am. Chem. Soc. **123**, 8844 (2001).
[44] J. Aldana, N. Lavelle, Y. Wang, and X. Peng, J. Am. Chem. Soc. **127**, 2496 (2005).
[45] See EPAPS supplementary material at http://dx.doi.org/10.1063/1.3251774 for additional depictions of the molecules and additional data tables referenced in the text.